Supplementary material for:

Title: *Atmospheric fluorescent bioaerosol concentrations measured during 18 months in a coniferous forest in the south of Sweden*

Authors:
Madeleine Petersson Sjögren[1], Malin Alsved[1], Tina Šantl-Temkiv[2], Thomas Bjerring Kristensen[3], Jakob Löndahl[1*]

[1]Department of Design Sciences, Faculty of Engineering, Lund University, Lund, Sweden
[2]Department of Biology, Microbiology Section and iCLIMATE Aarhus University Interdisciplinary Centre for Climate Change, Aarhus University, Aarhus, Denmark
[3]Department of Physics, Faculty of Engineering, Lund University, Lund, Sweden

Corresponding author: Jakob.Londahl@design.lth.se

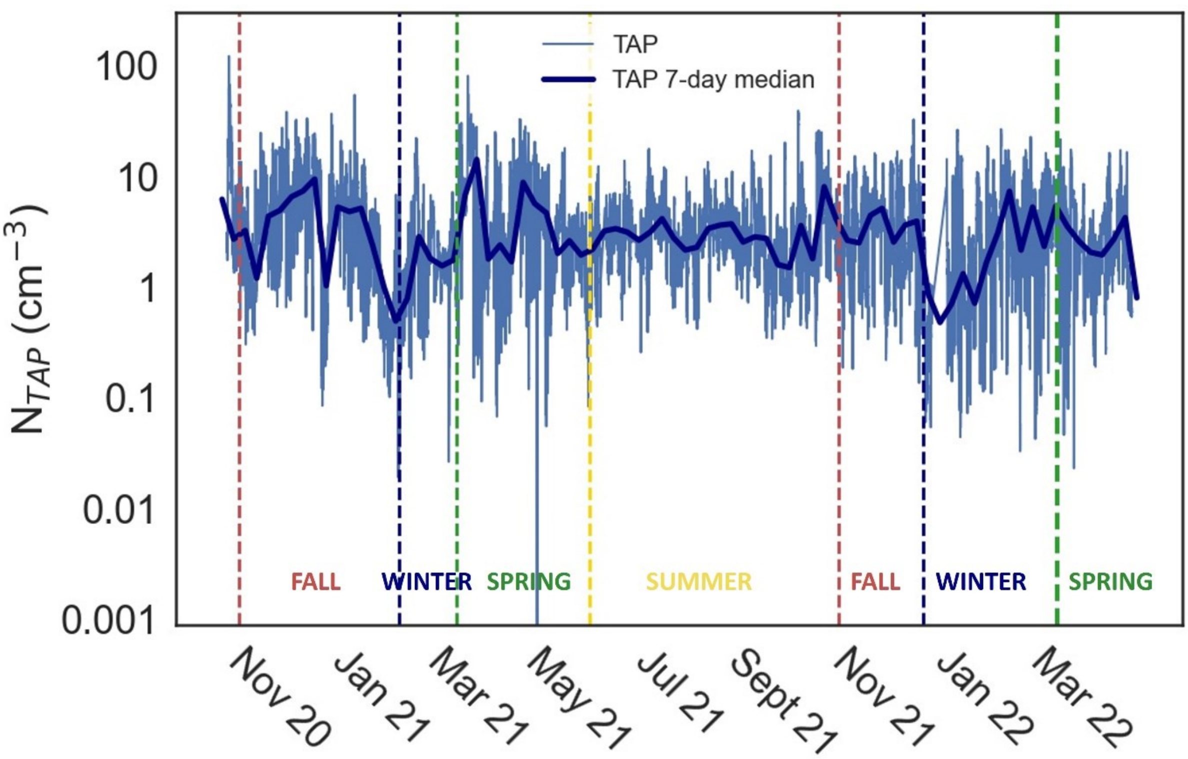

Figure S1: Overview of N_{TAP} concentration between 6 October 2020 and 1 April 2022. Small dots represent individual 5 min data averages. The curve cutting through the N_{TAP} data shows running 7-day median values of the N_{FBAP} concentration. Vertical dashed lines indicate the first day of each season as identified by the Swedish meteorological and hydrological institute.

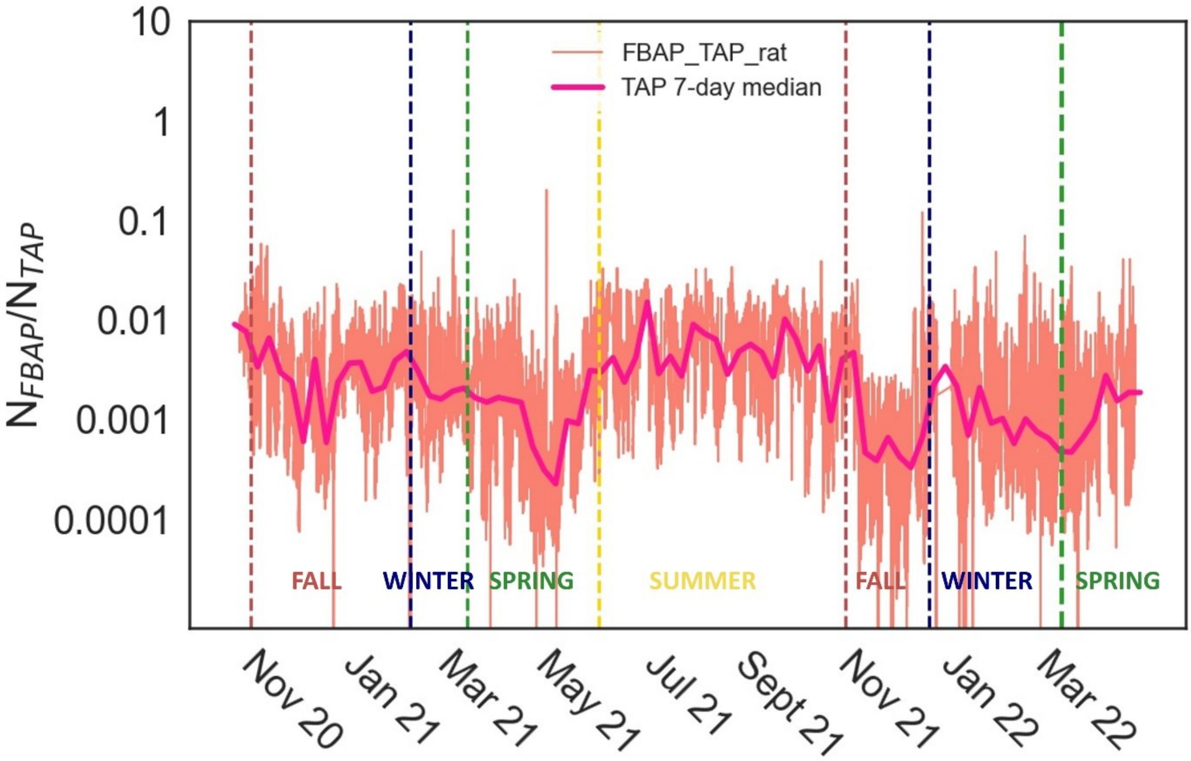

Figure S2: Overview of N_{FBAP}/N_{TAP} between 6 October 2020 and 1 April 2022. Small dots represent individual 5 min data averages and the curve cutting through the N_{FBAP}/N_{TAP} data shows running 7-day median values of the N_{FBAP}/N_{TAP}. Vertical dashed lines indicate the first day of each season as identified by the Swedish meteorological and hydrological institute. Overall, these data follow the general pattern of the N_{FBAP} with a steep increase at the intersection of spring and summer and steep decrease in the beginning of fall in 2021.

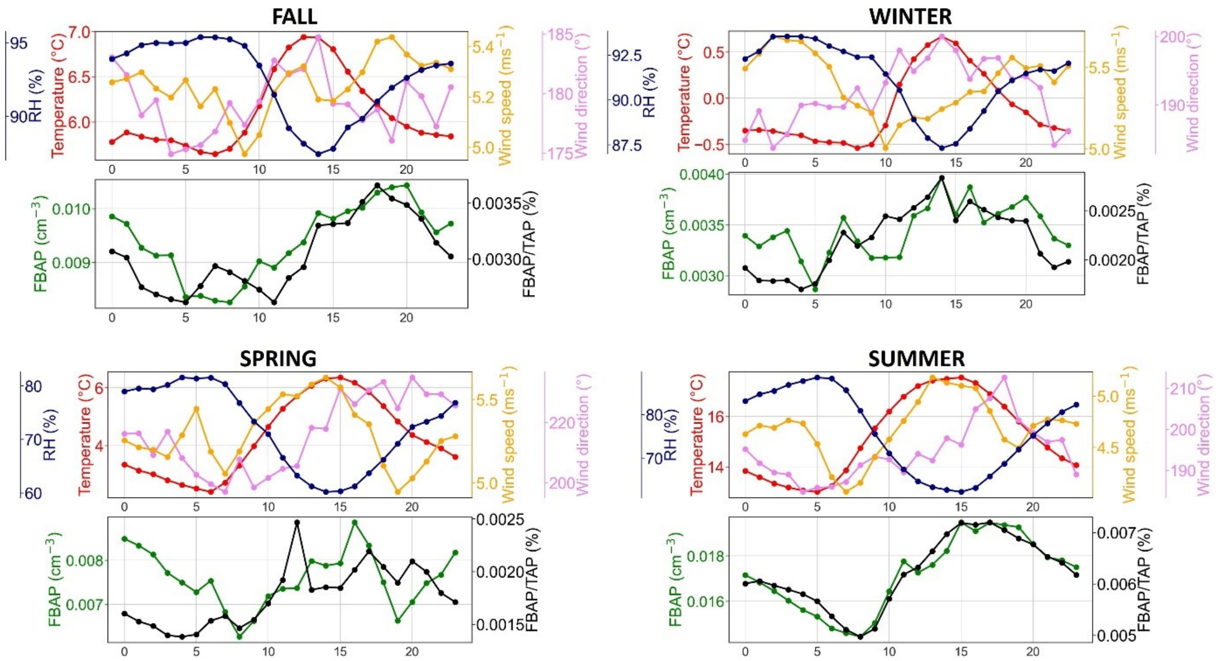

Figure S3: Diel cycles of meteorological parameters (top panels) and FBAP number concentrations with FBAP/TAP (lower panels) for each season of the measurement period (hourly median values as a function of local time of the day. In the top panel, left axis show air temperature and RH variations in and blue, while scales for wind speed and wind direction are indicated in yellow and pink. On the lower panels, the left axis shows integrated coarse FBAP concentration (green), while the right axis shows FBAP fraction of TAP number (black).

Figure S3 suggests that there are daily cycles for N_{FBAP} and N_{FBAP} / N_{TAP}, but the hourly and daily variations were numerically very small. This can be seen by investigating the leftmost y-axes in the lower panels in Figure S3. The seasonally averaged diurnal plots shown in Figure S3 indicate that for all seasons the minimum N_{FBAP}, and $N_{FBAP/TAP}$, occurred in the morning between 05:00 and 10:00. These cycles are somewhat in contrast with similar studies [1-5], which reported N_{FBAP} and N_{FBAP}/N_{TAP} to peak late in the evening, night-time, or early morning, when RH is minimum. In this study, only the fall season agrees well with the daily cycle previously observed.

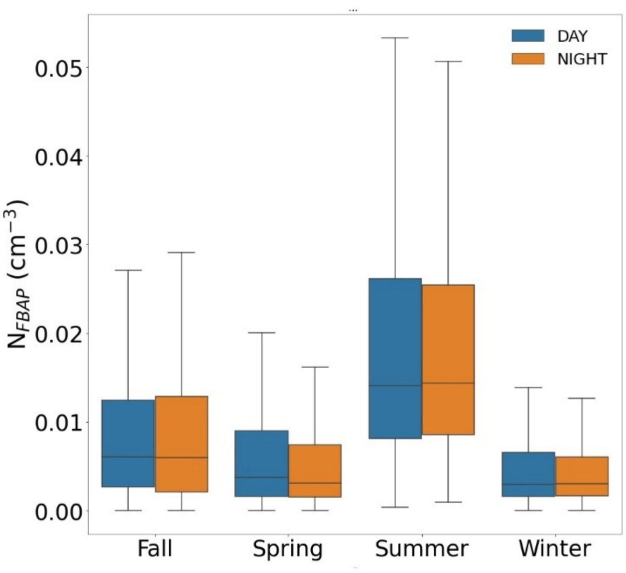

Figure S4: Statistical distributions of NFBAP abundance during daytime and nighttime over the full campaign, divided into each season. No difference was observed between N_{FBAP} during day as compared to night.

Figure S5 shows exemplary rain events in the fall (a) and in the summer (b). The left y-axis (red) shows the measured cumulative precipitation for each hour, while the right y-axis (black) shows N_{FBAP}. Each hour belonging to a rain event is marked with green, blue, and magenta depending on whether it counts as before, during or after rain. For each such an event one can see that increases in N_{FBAP} occurs, but it is also visible that similar such increases occur when there is no rain. It is also notable that the increases in N_{FBAP} seems to be related to the intensity of the rain, where a higher rain peak appears to induce a higher N_{FBAP} peak. Figure S6 displays the distribution of N_{FBAP} before, during, after rain and when there is no rain for each season. None of the distributions were statistically significantly different from each other.

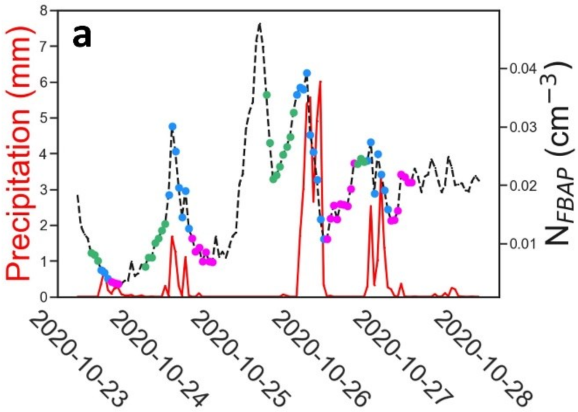

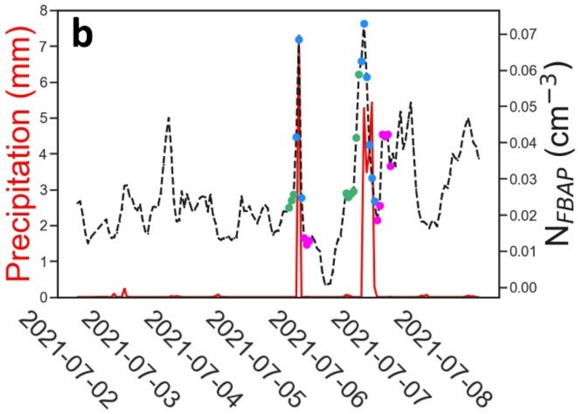

Figure S5: Two exemplary periods of time with rain events: 23-28 October 2020 (a) and 2-8 of July 2021. The cumulative hourly precipitation (red) is shown in red and the N_{FBAP} concentration is shown as the black dotted curve. Each consecutive hour with precipitation >0.5 mm was defined as a rain event. N_{FBAP} concentrations before (green), during (blue) and after (magenta) each rain event are indicated. Both periods in time indicate that in association with those rain events, an increase in N_{FBAP} was recorded. In addition to this, figure S6a seems so indicate that the increase in N_{FBAP} scaled with the intensity of the rain event.

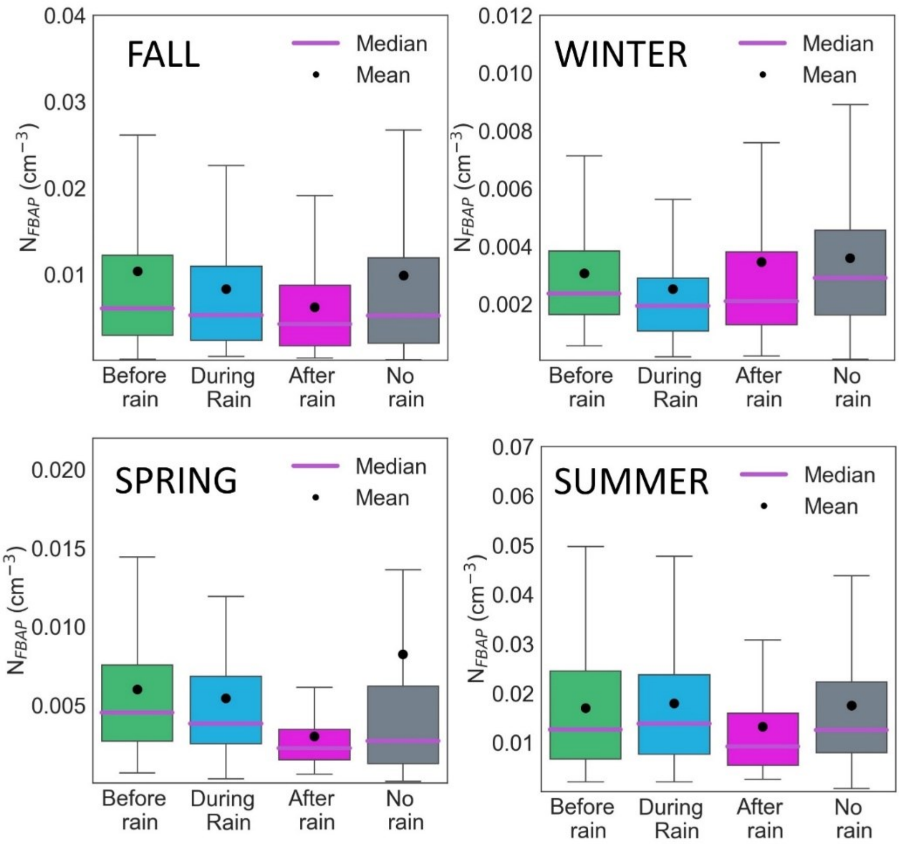

Figure S6: Integrated NFBAP concentrations for each season before, during, after and when no rain was measured. Although individual rain events were observed to cause strong increases in NFBAP, no significant effects were seen when integrating over the whole seasons.

Table S1: Extended version of table 1, also including shorter (≤ 4 weeks) LIF-FBAP measurements. Continuous measurements of FBAP with real-time detection, with identified associations and correlations with meteorological parameters and cycles in N_{FBAP}. When no average N_{FBAP} or N_{FBAP}/N_{TAP} was reported this is indicated by a hyphen. When both mean and median values were reported, they are here listed as mean/median.

Location	Land use	Instrument	Measurement period	Season(s)	Average N_{FBAP} (cm^{-3}) (Mean/ Median)	N_{FBAP} % of supermicron particles	Associations between FBAP and meteorology observed	N_{FBAP}-cycles
Mainz, Germany[1]	Semi-urban	UV-APS	4 months: Aug-Dec, 2006	Fall Winter	0.03	~4	FBAP increase with RH. No correlation with WD.	24-h cycle with max early/mid-morning
Amazon, Brasil[2]	Tropical rainforest	UV-APS	5 weeks: Feb-Mar, 2008	Rain season	0.073	24	FBAP increased with RH. FBAP decreased with AT Heavy rain was associated with FBAP increases.	24-h cycle with max in the night
Colorado, USA[3]	Semi-arid, rural forest	UV-APS WIBS-4	5 weeks: Jul-Aug, 2011	Summer	-	-	FBAP increased during rain	-
Hyytiälä, Finland[4]	Rural forest	UV-APS	20 months: Aug 2009-April 2011	Spring Summer Fall Winter	0.015 0.046 0.027 0.004	4.4 13 9.8 1.1	FBAP scaled with RH in summer in both locations. In Finland, at RH>82% FBAP decreased.	24-h cycle with max evening/night for all seasons.
Colorado, USA[4]	Semi-arid, rural forest.		11 months: Jul 2011-May 2012	Spring Summer Fall Winter	0.015 0.030 0.017 0.0053	2.5 8.8 5.7 3.0	FBAP increased upon rain events. FBAP increases with temp over seasons. No pattern seen for wind speed or wind direction.	
South-Western Germany5	Semi-rural	WIBS-4	1 year: April 2010-April 2011	Spring Summer Fall Winter	0.029/ 0.024 0.046/ 0.040 0.029/ 0.023 0.019/ 0.017	7/5 10/9 7/6 3/4 7/5		24-h cycle with max late evening/early morning.

					Full year: 0.031/ 0.025			
Helsinki, Finland[6]	Suburban and urban	BioScout UV-APS	3 weeks: Feb, 2012 9 weeks: Jun-Aug, 2012	Winter	0.010	5	-	24-h cycle with max in the night during summer.
				Summer	0.028	23		
Colorado, USA[7]	Semi-arid rural forest.	UV-APS WIBS-3	5 weeks: Jul-Aug, 2014	Summer	-	-	-	-
Munnar, India[8]	Tropical, high altitude.	UV-APS	11 weeks: June-Aug, 2014	Monsoon and winter*	0.02	2	FBAP strongly dependent on WD. FBAP increased with RH. FBAP decreased with AT. FBAP decreased with WS.	24-h cycle with max at high RH and low AT.
Manchester, UK[9]	Urban city center	WIBS-3	2 weeks: Dec, 2009	Winter	-	-	-	-
Borneo, Malaysia[9]	Remote, tropical		3 weeks: June-July 2008	Summer	-	-	-	-
Puy de Dôme, France[10]	Remote	WIBS-3	2 weeks: Jun-Jul,2010	Summer	0.27	-	-	24-h cycle with max mid-day.
Colorado, USA[11]	Semi-arid, rural forest	WIBS-3 WIBS-4	2 weeks: Jun-Jul, 2011	Summer	0.050-0.30	-	FBAP increased with RH.	24-h cycle with min at mid-day.
Killarney National Park, Ireland[12]	Rural	WIBS-4, UV-APS	4 weeks: Aug-Sep, 2010	Summer	-	-	FBAP increased with RH.	24-h cycle with max at night.
Nanjing, China[13]	Suburban	WIBS-4	2 weeks: Oct-Nov, 2013	Fall	0.57, 3.35, 2.09	4.6 25.3 15.6	-	-

[1,2,3] Huffman et al. (2010, 2012, 2013); [4] Scumacher et al (2013); [5] Toprak and Schnaiter (2013); [6]Saari et al. (2015); [7]Gosselin et al. (2016); [8]Valsan et al. (2016), [9,10] Gabey et al. (2011, 2013); [11] Crawford et al. (2014); [12] Healy et al. (2014); [13]Yu et al. (2016).
*Results were only reported for Monsoon period and not for the winter
Abbreviations: Relative humidity RH; Air temperature AT; Wind direction WD; Wind speed WS.

References

[1] J. A. Huffman, B. Treutlein, and U. Pöschl, "Fluorescent biological aerosol particle concentrations and size distributions measured with an Ultraviolet Aerodynamic Particle Sizer (UV-APS) in Central Europe," *Atmos. Chem. Phys.,* vol. 10, no. 7, pp. 3215-3233, 2010, doi: 10.5194/acp-10-3215-2010.

[2] J. A. Huffman, B. Sinha, R. M. Garland, A. Snee-Pollmann, S. S. Gunthe, P. Artaxo, S. T. Martin, M. O. Andreae, and U. Pöschl, "Size distributions and temporal variations of biological aerosol particles in the Amazon rainforest characterized by microscopy and real-time UV-APS fluorescence techniques during AMAZE-08," *Atmos. Chem. Phys.,* vol. 12, no. 24, pp. 11997-12019, 2012, doi: 10.5194/acp-12-11997-2012.

[3] C. J. Schumacher, C. Pöhlker, P. Aalto, V. Hiltunen, T. Petäjä, M. Kulmala, U. Pöschl, and J. A. Huffman, "Seasonal cycles of fluorescent biological aerosol particles in boreal and semi-arid forests of Finland and Colorado," *Atmos. Chem. Phys.,* vol. 13, no. 23, pp. 11987-12001, 2013, doi: 10.5194/acp-13-11987-2013.

[4] E. Toprak and M. Schnaiter, "Fluorescent biological aerosol particles measured with the Waveband Integrated Bioaerosol Sensor WIBS-4: laboratory tests combined with a one year field study," *Atmos. Chem. Phys.,* vol. 13, no. 1, pp. 225-243, 2013, doi: 10.5194/acp-13-225-2013.

[5] S. Saari, J. Niemi, T. Rönkkö, H. Kuuluvainen, A. Järvinen, L. Pirjola, M. Aurela, R. Hillamo, and J. Keskinen, "Seasonal and Diurnal Variations of Fluorescent Bioaerosol Concentration and Size Distribution in the Urban Environment," *Aerosol and Air Quality Research,* vol. 15, no. 2, pp. 572-581, 2015, doi: 10.4209/aaqr.2014.10.0258.